

Stein-based Optimization of Sampling Distributions in Model Predictive Path Integral Control

Jace Aldrich

Odest Chadwicke Jenkins

Abstract—This paper presents a novel method for Model Predictive Path Integral (MPPI) control that optimizes sample generation towards an optimal trajectory through Stein Variational Gradient Descent (SVGD). MPPI is traditionally reliant on randomly sampled trajectories, often by a Gaussian distribution. The result can lead to sample deprivation, under-representing the space of possible trajectories, and yield suboptimal results. Through introducing SVGD updates in between MPPI environment steps, we present Stein-Optimized Path-Integral Inference (SOPPI), an MPPI/SVGD algorithm that can dynamically update noise distributions at runtime to shape a more optimal representation without an excessive increase in computational requirements. We demonstrate the efficacy of our method systems ranging from a Cart-Pole to a two-dimensional bipedal walking task, indicating improved performance above standard MPPI across a range of hyper-parameters and demonstrate feasibility at lower particle counts. We discuss the applicability of this MPPI/SVGD method to higher degree-of-freedom systems, as well as its potential to new developments in state-of-the-art differentiable simulators.

Index Terms—Variational inference, planning as inference, model predictive control

I. INTRODUCTION

Model Predictive Control (MPC) methods, along with other optimal control methods, have become commonplace in several domains for robotics, ranging from simple automotive to even high-degree-of-freedom humanoid robots. The space of MPC-based methods includes an information theoretic nonparametric sampling method, Model Predictive Path Integral Control (MPPI) [1]. While the performance of MPPI, both in resultant trajectories and computation time, is stellar, this form of control often remains limited to relatively low-dimensional spaces or is abstracted to a lower dimension to make the problem more feasible. We aspire to realize MPPI methods suitable for real-time robust inference for more complex robotic platforms, such as humanoid robots.

The key concept of MPPI involves information maximization over a projected set of rollout trajectories [1]. From a current state estimate and initial action sequence, MPPI will heavily perturb the action sequence, generating a distribution of trajectories, which are then rolled out via state dynamics. MPPI then aims to minimize the Kullback–Leibler (KL) Divergence [2] (a measure of the difference between two distributions) between this distribution of rollouts and an optimal trajectory distribution, identified by a cost function.

J. Aldrich and O. C. Jenkins are with the Laboratory for Perceptive RObotics and Grounded REasoning SystemS and Robotics Department at the University of Michigan, Ann Arbor, USA. This work was supported in part by Amazon, Ford Motor Company, and a National Science Foundation Graduate Research Fellowship.

Functionally, this equates to performing an information maximization expectation to pick a trajectory which is a weighted sum of the sampled trajectories. The perturbations, however, are often generated from Gaussian distributions, which causes sampling to primarily explore around the mean, which is not often representative of the true optimal distribution [3]. Particularly for constrained high degree-of-freedom nonlinear systems, this MPPI algorithm becomes susceptible to the curse of dimensionality, requiring exponentially more samples to be effective [4].

For similar problems relating to gradient based optimization Stein Variational Gradient Descent (SVGD), or Stein Variational Inference [5] has become increasingly popular, wherein as part of an optimization step, a kernel is used to force particles to spread out. This kernel ensures a more complete representation of a sampled space and prevents mode collapse, often improving particle efficiency. There are several implementations of SVGD within MPC, highlighted by [6], and a few within MPPI [7], [8]. However, these representations each have their own issues. For strict MPC implementations, the kernel often loses meaning quickly as it must differentiate particles over several sets of dimensions (the horizon, number of rollouts, and state and/or action dimensions). These high dimensions often make kernel distances much more arbitrary, limiting the effectiveness of the repulsive kernel force in SVGD. Additionally, the Stein component of the gradient descent update must often be recursively updated through the cost functions and dynamics over the entire horizon, adding significant computation time. There have been attempts to merge SVGD with MPPI as well [7], [8], however, for the aforementioned reasons, they perform SVGD on simplistic systems, velocity-input models, or a small subset of particles, which can minimize SVGD’s impact.

In this paper, we present Stein-Optimized Path-Integral Inference (SOPPI), an algorithm that combines SVGD with MPPI, operating within the action space of the inference model to improve sampling over baseline MPPI. We study the cart-inverted-pendulum (cart-pole) system to demonstrate operation in unstable, erratic systems and study the effects of particle counts and sample efficiency between the algorithms. Our findings from these tests suggest that there is a statistically significant improvement at the 95% level in SOPPI’s effectiveness over baseline MPPI, even when operated at lower particle counts. We also study higher degree-of-freedom (DOF) systems: a block pushing task with a 7-DOF robotic arm and a two-dimensional bipedal locomotion task with a 7-link, 6 DOF walking robot. These

systems further allude to SOPPI’s improved performance over MPPI with respect to targeted control metrics. As a whole, the experiments demonstrate that SOPPI outperforms MPPI by generating samples that more effectively cover the solution space to the given control problem.

II. RELATED WORK

A. MPC Methods

Model Predictive Control (MPC) represents a collection of controller types that optimize trajectories via an explicit model [9]. One of the most common MPC methods is under direct optimization, for example, forming a quadratic programming problem over a system’s state space to minimize some cost function. These methods function on both linear and non-linear systems, although linear models are simpler and much more consistent. [10]. MPPI, on the other hand, is a sampling-based approach for stochastic trajectory optimization, as introduced by Williams et. al in [1]. MPPI algorithms generate several sample trajectories that are evaluated and weighted to minimize the cost function instead.

B. MPPI Enhancements

Several versions of MPPI expand upon the original work [1]. In particular, Tube MPPI [11] runs multiple controller layers to create more trajectory guarantees. Constrained Covariance Steering MPPI [12] builds upon this further, adding covariance tracking to Tube MPPI. Robust MPPI [13] introduces additional safeties and disturbance rejection by importance sampling and augmented state spaces. Reinforcement Learning (RL) MPPI methods [14], [15] attempt to improve sample efficiency though reinforcement learning by training an agent to generate trajectories, instead of baseline MPPI’s normal distribution sampling. However, these methods suffer from normal RL drawbacks such as training data, time, and constraints. Unscented MPPI [4] implements an Unscented Transform to help manage uncertainty during rollouts, propagating mean and uncertainty throughout sampling. There are several other methods of MPPI with their own improvements, but the aforementioned versions cover the space of MPPI methods at a high level.

C. Gradient Descent Optimizations

On the other end of optimization lie gradient descent methods, in particular, stochastic variational inference [16]. This method operates in the probability space, and optimizes some distribution to an optimal distribution via gradient-based update rules and minimizing KL-divergence, a measure of the difference between two distributions. Stein Variational Gradient Descent (SVGD) [5] is a variation of that method that applies update rules as in variational inference, but also with kernel terms. These terms encourage particles to avoid mode collapse, increasing particle efficiency and assisting in multi-modal distributions.

Bringing SVGD and MPC together is Stein MPC [6], which treats MPC as a Bayesian inference problem (as many other methods do). This combination allows the application of SVGD instead of traditional gradient descent,

which assists in complexity and multi-modality in trajectory selection. However, both represented in this work and the Authors’ own attempts [6], implementing a kernel across a high dimension, long horizon problem with a large number of samples quickly makes the kernel lose meaning. The extremely high dimensionality asks the kernel to cover too large of a solution space, which reduces the overall coverage of the method. Hence, Stein MPC scales less effectively with respect to solution space coverage if the kernel is applied over the entire problem.

There are several further works [17], [18] that implement SVGD as well, focusing on the trajectory optimization problem, and works which implement SVGD in a belief propagation algorithm [19], [20], similar to Stein MPC.

D. Differentiable Dynamics

As with most optimization methods, SVGD requires gradient computations to function. With modern automatic differentiation in tools such as PyTorch [21], this process is quite simple for analytical dynamics. However, more complex systems require significant modeling, which can create lengthy and complicated dynamic functions. For this reason, many simulation tools such as MuJoCo [22] and Gymnasium [23] are commonplace, however, they are often non-differentiable. Differentiable simulation is an active field with many aspiring candidates, but several have key limitations including simplified operations and below real-time runtime [24]. Platforms such as Google’s Brax [25] and NVIDIA’s Warp [26] are promising, but introduced computational stability issues during the sampling and resetting requirements of our implementations of MPPI and SOPPI. For these reasons, this paper utilizes recurrent neural networks [27] to approximate gradients of the dynamics function when required, but hopes to implement these differentiable simulators in the future.

III. METHODS

A. MPPI

In this paper, we build upon the original derivation of MPPI in [1]. We consider the stochastic optimal control problem for the general, discrete-time dynamic system operating in a continuous space

$$x_{t+1} = F(x_t, v_t)$$

where x_t, v_t represent system state and controls at time t and F denotes the system dynamics. Additionally, v_t is assumed to be normally distributed $v_t \sim N(u_t, \sigma^2)$ where u_t represents a targeted input, and σ^2 represents some process noise. We then aim to optimize some control trajectory $U = (u_0, u_1, \dots, u_{T-1})$ of length T via

$$U^* = \arg \min_{U \in \mathbb{U}} \mathbb{E} \left[\phi(x_T) + \sum_{t=0}^{T-1} \mathcal{L}(x_t, u_t) \right]$$

where $\mathcal{L}(x_t, u_t)$ and $\phi(x_T)$ represent running and terminal cost functions respectively, defined as

$$\mathcal{L}(x_t, u_t) = x_t^T Q x_t^T + u_t^T R u_t \quad (1)$$

$$\phi(x_T) = x_T^T Q_T x_T \quad (2)$$

where R, Q, Q_T represent weight matrices for action costs, running state costs, and terminal state costs. We can then define $S(\tau)$, a cost-to-go function, as dependent on an entire trajectory such that

$$S(\tau) = \phi(x_T) + \sum_{t=0}^{T-1} L(x_t, u_t) \quad (3)$$

where τ represents a trajectory in the form

$$\tau = (x_0, u_0, x_1, u_1, \dots, x_T)$$

To optimize, we first must generate a set of K sample trajectories to minimize KL-Divergence towards some optimal trajectory. This process is done by sampling a zero-mean gaussian noise ε with some variance σ^2 , and adding it to some initial guess of a trajectory u . These trajectories are rolled out and have their costs computed. Then, the original MPPI derivation yields that for these sample trajectories, each with its own cost-to-go, we can approximate u^* via an iterative update for K samples

$$u^* = u + \sum_{k=1}^K w_k \varepsilon^k \quad (4)$$

where w_k represents a weight for the k th trajectory with cost S_k , solved as

$$w_k = \frac{\exp(-\frac{1}{\lambda}(S_k - \beta))}{\sum_{j=1}^K \exp(-\frac{1}{\lambda}(S_j - \beta))} \quad (5)$$

where $\beta = \min_{k \in \mathbb{K}}(S_k)$. Note that there are several MPPI variations that apply filtering to the update step as well, which in some cases may improve system performance.

B. SVGD

Similar to MPPI, SVGD also attempts to optimize some particle set to an optimal state by minimizing KL-Divergence. For a set of particles $\{\theta^i\}_{i=1}^k$ It follows the iterative update rule of

$$\theta^i \leftarrow \theta^i + \epsilon \phi^*(\theta^i)$$

where ϵ represents a step size, and $\phi^*(\cdot)$ defines the optimal perturbation to reduce KL-divergence via kernel functions, and can be approximated for a set of K particles via

$$\hat{\phi}^*(\theta) = \frac{1}{K} \sum_{j=1}^K [k(\theta^j, \theta) \nabla_{\theta^j} \log p(\theta^j || x) + \nabla_{\theta^j} k(\theta^j, \theta)] \quad (6)$$

where $k(\cdot)$ represents a valid kernel function. Essentially, the first term is a scaled gradient log-likelihood of the particle's posterior, which drives the particles towards an optimal state. The second term is a repulsive force, preventing mode collapse and allowing greater coverage of the sample space. A full derivation can be found at [5], with a high-level explanation at [6].

C. SOPPI

Similar to [7], the SOPPI method (Algorithm 1) we propose performs SVGD updates to improve the random samples generated for MPPI. In theory, performing SVGD is possible over the entirety of all generated trajectories, however, this process would be highly computationally expensive, requiring differentiation over a large computational graph of dynamics. Instead, we optimize the noise added to the distribution, which greatly simplifies the computation required. SOPPI uses the same cost structure as normal implementations of MPPI as seen in Equations 1 and 2. Similiar to Miura et al. [7], we interweave SVGD updates to the trajectories throughout the process; however, in our case, we apply SVGD updates online.

To start, SOPPI performs a single step of MPPI (i.e., one timestep in the environment) to gain a set of samples for one time step. SVGD is then applied to that step's samples to optimize their distribution to an optimal cost state for a single time step. Specifically, SOPPI uses the same cost as our base MPPI implementation, Equation 3, however, for all but the last time-step, the terminal cost is undefined. So, the cost function reverts to Equation 1, as we currently only evaluate one time-step at a time for SVGD updates.

Performing these updates over only a single time step instead of the entire horizon serves a few purposes. First, it keeps the gradient calculations computationally efficient and stable, as often times long-horizon problems will suffer from exploding or vanishing gradients. Second, it allows the kernel operation from SVGD to maintain its meaning, as we reduce the dimensionality it is required to cover. By envisioning the SVGD computation as a series of small sub-problems at each timestep, we can ensure that the kernel operation appropriately prevents mode collapse. Thus, this method can improve sampling efficiency from the standard normal distribution sample. Lastly, performing single step updates in this manner allows the subsequent step to benefit from the improved sampling. Attempting to update every timestep at once can hinder convergence as it vastly increases the number of dimensions to search over at once.

After these updates, we can derive a cost-likelihood function \mathcal{L}_s for SOPPI from the MPPI costs to represent our trajectory's distribution, such that

$$\mathcal{L}_s(x_t, u_t) = \exp(-\alpha \mathcal{L}(x_t, u_t)) \quad (7)$$

Thus, the gradient of the log likelihood as listed in Equation 6 is simply the negative scaled gradient of our cost function. Additionally, we use a standard radial-basis (RBF) kernel parameterized by σ defined as

$$k(v_t^j, v_t) = \exp\left(-\frac{\|v_t^j - v_t\|}{2\sigma^2}\right) \quad (8)$$

From these equations, we compute the SVGD update for SOPPI defined in 6, and apply it to the sampled action particles. Then, we re-compute the rollout with the new actions, continuing the MPPI process as normal. This process is repeated throughout the chosen horizon, after which the

standard weighting defined in MPPI's equations 4 and 5 are used to select an optimal trajectory. The entire algorithm is depicted in Algorithm 1.

Algorithm 1: SOPPI

Data: K : Number of samples
 N : Number of timesteps
 M : Number of SVGD Updates
 U_{init} : Initial control sequence
 $f(x, u)$: Dynamics function
 $k(v, v)$: Kernel function
 σ^2 : Sampling variance
 λ : Temperature parameter

```

while task not completed do
     $\epsilon \sim \mathcal{N}(0, \sigma^2)$ ;
     $v \leftarrow U_{init} + \epsilon$ ;
    for  $k \leftarrow 0$  to  $K - 1$  in parallel do
         $x^k \leftarrow x_0$ ;
         $S^k \leftarrow 0$ ;
        for  $t \leftarrow 0$  to  $N - 1$  do
            for  $i \leftarrow 0$  to  $M - 1$  do
                 $x_{t+1}^k \leftarrow f(x_t^k, v_t^k)$ ;
                 $S_s^k \leftarrow \mathcal{L}(x_t^{k+1}, v_t^k)$ ;
                 $\hat{\phi}^*(v) \leftarrow \frac{1}{K} \sum_{j=1}^K [-k(v^j, v) \nabla_{v_t^k} S_s^k + \nabla_{v^j} k(v^j, v)]$ ;
                 $v_t^k \leftarrow v_t^k + \epsilon \hat{\phi}(v)$ ;
                 $x_{t+1}^k \leftarrow f(x_t^k, v_t^k)$ ;
                 $S^k \leftarrow S^k + \mathcal{L}(x_t^{k+1}, v_t^k)$ ;
             $S^k \leftarrow S^k + \phi(x_N^k)$ ;
             $\beta \leftarrow \min_{k \in \mathbb{K}}(S_k)$ ;
             $w_k \leftarrow \frac{\exp(-\frac{1}{\lambda}(S_k - \beta))}{\sum_{j=1}^K \exp(-\frac{1}{\lambda}(S_j - \beta))}$ ;
             $u^* \leftarrow u + \sum_{k=1}^K w_k \varepsilon^k$ ;
             $x_0 \leftarrow f(x_0, u_0^*)$ ;
             $U_{init} \leftarrow [u_{1:N}^* \ 0]$ ;

```

IV. EXPERIMENTS

We conducted a series of simulation experiments on analytically derived dynamics, comparing SOPPI vs baseline MPPI for multiple tasks: a single DOF cart-pole upswing, 7-DOF robot arm box pushing, and a planar 6-DOF bipedal walking. All simulations were conducted through Pytorch [21] and analytical dynamics or the Gymnasium [23] wrap of MuJoCo [22] with a trained recurrent neural network. All tests were performed with a i7-13700K CPU, accelerated by a Nvidia A6000 GPU.

A. Cart Pole

For the cart-pole swing-up task, we used an analytical dynamics model [28] where the upright position was defined as a pole angle of $\theta = 0$, and starting downward position as $\theta = \pi$, with the cart's position starting and ending at $x = 0$.



Fig. 1. Cart-pole system. Initial state of $x = 0, \theta = \pi$ (left). Target state of $x = 0, \theta = 0$ (right). Visualization code provided by [29].

A brief visualization of the cart-pole system is depicted in Figure 1.

We performed a range of tests on both MPPI and SOPPI, with different hyper-parameters, focusing on sample count and horizon timesteps. From these tests, we determined a horizon of 80 time steps, or 1.6 seconds as an appropriate, and present results at 500 and 1000 particles to demonstrate differences in particle efficiency between the two algorithms. In the presented data, all hyper-parameters and costs were identical, with only horizon and sample counts varying. Additionally, for the SOPPI algorithm, we performed tests with multiple variations of learning rates and iterations, but present nominal values with a learning rate of 0.05 over 100 time steps. All numerical results from these tests can be noted in Table I depicting settling times t_s for both x and θ for multiple criteria (for example, 0.25 m on x or 5% of the θ range), and Figure 2 depicts visual results. Additionally, Table I contains P-values from a Welch's t-test, indicating statistical results between the trials.

From these results, we note that SOPPI in both cases performs approximately equal to or better than MPPI. In particular, our mean squared error from the desired position and the settling time to it is reduced by SOPPI at an equal particle count trial of MPPI. Effectively, this implies that, on average, SOPPI is driving particles towards their optimal state as dictated by our cost function, thus improving sampling over baseline MPPI.

For settling time on the cart's position, we see two trends. For the 0.25 meter criteria, we note an increase in significance as particles increase, although the 500 particle case had outliers which may skew the results. However, the more interesting trend relates to the 0.5-meter settling time. There is a sharp increase in performance at 500 particles compared to 1,000 particles, suggesting an optimal point relating to particle count and kernel repulsion. Comparing the 0.5 meter settling time for SOPPI between the 500 and 1,000 particle cases, we note nearly a standard deviation of an increase, suggesting that at these particle counts, the kernel from SVGD may be too heavily penalizing solutions. This trend is further reinforced by the pole angle (θ) settling times.

Specifically, for SOPPI, we can note that all angle settling time means for the 500 particle count case are less than or equal to the 1,000 particle case for both MPPI and SOPPI. Effectively, we demonstrate that the SVGD updates are indeed optimizing the sample distributions, generating better results at lower particle counts than baseline MPPI.

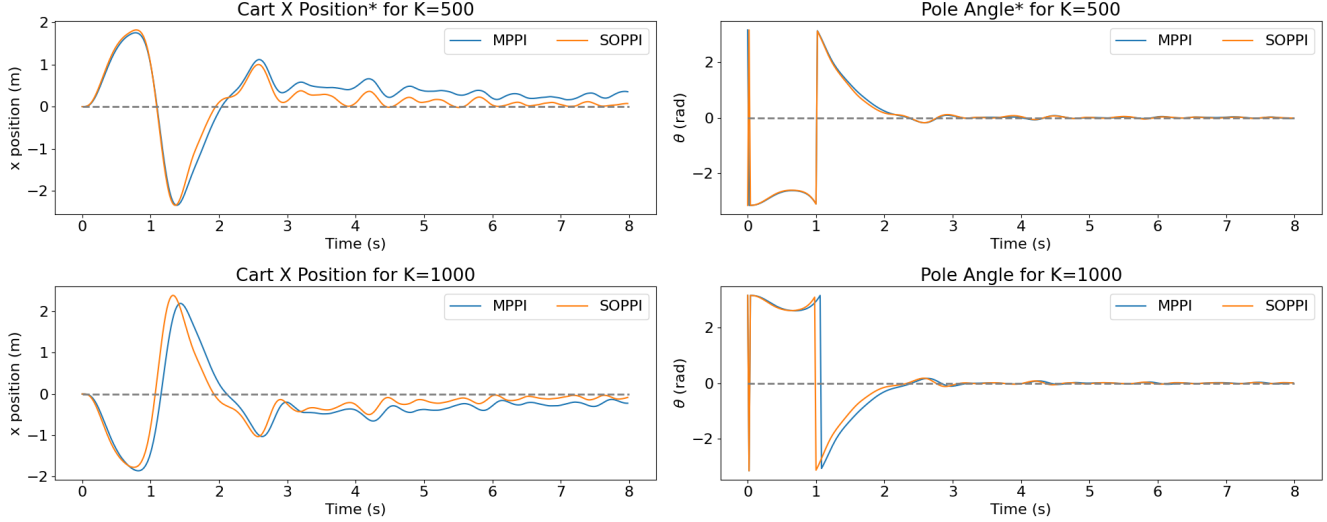


Fig. 2. Cart-Pole response for a horizon (H) of 80 steps (1.6 seconds) and 500 and 1,000 particles (K).

TABLE I

CART INVERTED PENDULUM SYSTEM RESPONSE FOR A HORIZON (H) OF 80 STEPS OR 1.6 SECONDS, AND VARIOUS PARTICLE COUNTS (K). STATISTICALLY SIGNIFICANT (95%) RESULTS ARE BOLDED.

Trial	MSE(x)	$t_{s,x,0.25m}$	$t_{s,x,0.5m}$	MSE(θ)	$t_{s,\theta,2\%}$	$t_{s,\theta,5\%}$	$t_{s,\theta,10\%}$
MPPI H=80, K=500	0.58	$6.77 \pm 0.94^\dagger$	4.33 ± 0.02	1.36	4.16 ± 0.61	2.68 ± 0.02	1.97 ± 0.02
SOPPI H=80, K=500	0.53	$5.20 \pm 0.80^\dagger$	3.46 ± 0.73	1.29	4.05 ± 0.57	2.65 ± 0.02	1.87 ± 0.04
P-value (SOPPI better than MPPI)	0.004	0.022	0.028	0.002	0.391	0.006	0.001
MPPI H=80, K=1,000	0.56	6.64 ± 0.69	4.03 ± 0.68	1.36	4.34 ± 0.10	2.69 ± 0.01	1.98 ± 0.02
SOPPI H=80, K=1,000	0.53	5.66 ± 0.51	3.93 ± 0.66	1.30	4.35 ± 0.14	2.65 ± 0.01	1.87 ± 0.01
P-value (SOPPI better than MPPI)	0.010	0.019	0.413	0.0001	0.560	0.0001	0.000003
P-value (SOPPI K=500 better than MPPI K=1,000)	0.031	0.003	0.322	0.003	0.002	0.029	0.238

Note: $t_{s,x}$ and $t_{s,\theta}$ represent settling times of x and θ , followed by criteria: a meter range for x or percentage of the step range (π) for θ .

* One out of five trials did not converge; † Two out of five trials did not converge; - Three or more trials did not converge

These results from the cart-pole system were used to validate the algorithm design, and provide insight to testing further systems.

B. Arm Pushing Task

To increase the complexity of the system over the cart-pole, we elected to test the algorithm on a simulated planar pushing task on a block with a Franka Panda arm based on Berenson et al. [30]. To simplify the dynamics at runtime while maintaining gradients, we trained a recurrent neural network [27] to approximate the dynamics from a MuJoCo simulation. In this formulation, states represent the block's pose $\mathbf{x} = [x \ y \ \theta]^\top \in \text{SE}(2)$ and actions $\mathbf{u} = [p \ \phi \ \ell]^\top \in \mathbb{R}^3$ are represented by p corresponding to the lower edge pushing location of the block, ϕ corresponding to the pushing angle, and ℓ corresponding to the pushing length as a fraction of the maximum allowed length (0.1 m in this case). In all tests, the arm was tasked with pushing the block from the pose $[0.4, 0, \frac{\pi}{5}]$ to $[0.8, 0, 0]$.

Since this task was inherently more stable than the cart-pole task, we elected for a shorter horizon and number of samples, 10 time steps or 0.2 seconds and 100 samples, for

both MPPI and SOPPI. We performed significantly more optimization steps on SVGD updates, but with a learning rate of 0.15 over 100 steps, as the search space is inherently more stable than that of the cart-pole case. All other hyperparameters and cost functions were identical between trials for both MPPI and SOPPI. Table II and Figure 4 (the median error trial) depict numeric results, and Figure 3 depicts visuals of the state transitions.

TABLE II
STEADY STATE PUSHING TASK ERRORS BETWEEN DESIRED AND ACTUAL END POSES OF THE PUSHED BLOCK

Statistic	MPPI	SOPPI
End x Mean Error	34.2 mm	22.5 mm
End y Mean Error	65.6 mm	62.6 mm
End θ Mean Error	2.47 mm	4.67 mm
End x Standard Deviation	9.88 mm	10.7 mm
End y Standard Deviation	3.54 mm	5.84 mm
End θ Standard Deviation	1.74 mm	0.770 mm
End x Median Error	34.9 mm	24.4 mm
End y Median Error	65.9 mm	62.2 mm
End θ Median Error	2.87 mm	4.74 mm

Overall, from Table II we note that the mean and median

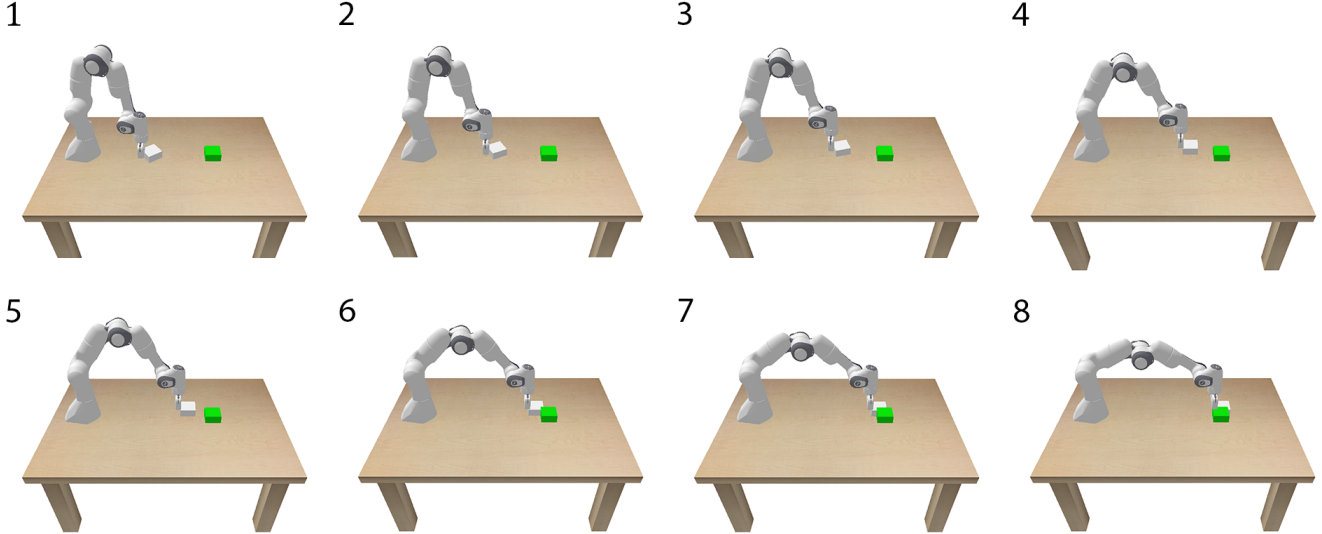


Fig. 3. Pushing task visualization of the Franka arm pushing a block (white) to a target pose (green). Events are sequenced in ascending numerical order.

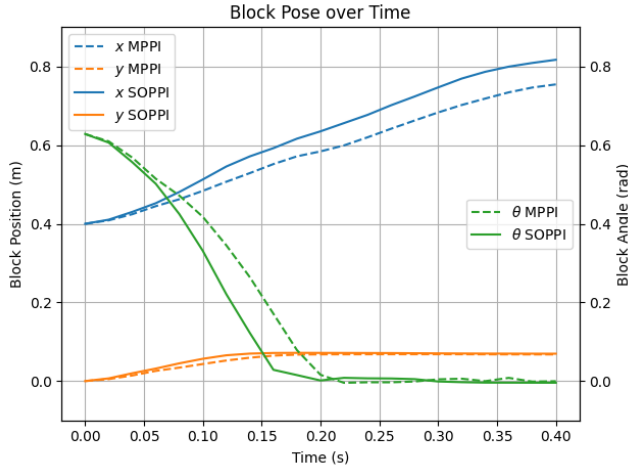


Fig. 4. Median mean squared error trial block pose response compared between MPPI and SOPPI. Time is paused when the arm is not in contact with the block.

steady-state response errors are considerably better on the x direction (the main pushing direction) with a slight overshoot noticeable in Figure 4. The y -direction is slightly better with SOPPI, and the block angle is slightly worse. However, from Figure 4, we can note that our transient responses are much better on both x and θ , with little difference in y . These trends are highly similar to those of the cart-pole case, where the system converges to its steady-state value faster, reducing error in a faster fashion with SOPPI compared to MPPI.

C. 2D Walker Task

Lastly, we implement SOPPI and MPPI on the Walker2D gymnasium environment [23], which is commonly used in the reinforcement-learning community. However, due to the unstable dynamics of the system's 6 joints, we implement a cost structure similar to [31], wherein we apply a reference

input trajectory around some known gait. Since this system is well studied in the RL community, we trained a Proximal Policy Optimization (PPO) [32] model to use as our reference gait, from the Stable Baselines3 package [33]. Additionally, our cost structure was modified from 1 to

$$\mathcal{L}(x_t, u_t) = x_t^T Q x_t^T + (u_t - u_{ref})^T R (u_t - u_{ref})$$

where u_{ref} was computed by the PPO model, rolling out from the current state with its own generated actions. During sampling, we also modified the initial input for the last time step to be the output of the PPO model at the next to last time step's states. So the last line of Algorithm 1 becomes

$$U_{init} \leftarrow [u_{1:N}^* \quad \text{PPO}(x_{N-1})]$$

To simplify gradient calculations as well, we trained another recurrent neural network to approximate the dynamics of the system for a single step (the duration of gradients required), but used MuJoCo simulations for rollouts, as given the chaotic nature of the walker robot, the neural network and MuJoCo results began to diverge beyond a few timesteps. This issue could be solved with longer training time and more data, allowing the walker to directly rely on a neural network, but was not required for SOPPI to function.

Lastly, we tweaked our cost matrix, Q to prioritize maximizing the height of the walker's torso, and added forward kinematic costs which incentivized the robot's feet to be further apart. Both modifications led to more stable, continued steps. We conducted eight trials for each algorithm with all hyper-parameters and cost functions equal (only adding the SVGD updates to SOPPI). We elected for a 50 time-step horizon and 1,000 samples for each case. The results of these trials are depicted in Table II and Figure 6 (the median length trial), with visuals of the system walking depicted in Figure 5. We consider the metric of "walking time" to denote the

stable duration, and consider the end of walking time as the last peak of torso height before the torso falls below 1 meter.

TABLE III
WALKER TASK WALKING TIME. LONGER TIMES INDICATE FURTHER
DISTANCE TRAVELED UPRIGHT

Statistic	MPPI	SOPPI
Mean Walking Time	20.37 s	44.41 s
Standard Deviation	13.33 s	24.83 s
Median Walking Time	15.20 s	39.49 s

In our experiments, we observe that on average, SOPPI trials were able to last the longer than the MPPI trials, although not indefinitely. Typically, a trial failed (denoted by the walker falling to the ground) by either a slip or stall in momentum, which we believe to be caused by failure to sample a valid trajectory. Thus, we believe that with the improved sampling of SOPPI, the walker is overall more stable and better able to maintain its upright position.

We do however, notice a large variance in the results for both algorithms, although conducting a one-tailed Welch's t-test on the walking times of both systems yields a p-value of 0.023, indicating a significant improvement at the 95% level on SOPPI over MPPI. We expect that this variance is due to the chaotic, unstable nature of the system. Similar to how we only used a neural network for model gradients (as opposed to the entire rollout) for stability, we expect that the sampling requirements for perfect stability are higher than conducted in our trials. In addition, many real-world systems and otherwise utilize less chaotic gaits than our chosen reference gait, which is more akin to a "skipping" motion than a walking one. For this reason, we expect that implementing SOPPI on systems designed for the real-world (whether in simulation or not), which have the benefit of tested, stable gaits, would reduce this variance. Instead, SOPPI would lead to more optimized gaits for specific situations (e.g., obstacles on the ground), rather than attempting to maintain a stable gait for an infinitely consistent task.

V. CONCLUSION AND FUTURE WORKS

In this paper, we presented SOPPI, a novel method that interweaves SVGD updates into MPPI, combining the benefits of SVGD's explicit optimization with reduced particles and MPPI's general computational simplicity. We performed a range of experiments including a cart-pole swing up, a block pushing task, and a two dimensional walking task, all demonstrating SOPPI's efficacy compared to baseline MPPI. Specifically, the SVGD updates within SOPPI optimized the noise typical in MPPI applications to generate an improved performance over baseline MPPI, even when in some cases where SOPPI had less particles than MPPI. With these results, we demonstrated that SOPPI effectively increases either the algorithm's performance, particle efficiency, or both, over baseline MPPI, paving the way for future works with higher-dimension systems.

In the future, we intend to expand this algorithm threefold. First, we plan to implement SVGD updates over a longer

sub-horizon, instead of just a single step. Ideally, we will find an effective tradeoff between computational complexity and improved sampling efficiency. Secondarily, we intend to expand this work to new developments in differentiable simulators, including NVIDIA Warp [26] and Brax [25] which would simplify our requirements for differentiable dynamics. Lastly, we aim to implement this work on more systems, specifically, higher dimensional walkers and real-world systems, such as the Agility Robotics Digit. In cases such as these, we additionally hope to implement multiple gaits and demonstrate abilities to switch between them, for example, a standing and walking gait, which would hold itself well to real-world applications.

REFERENCES

- [1] G. Williams, P. Drews, B. Goldfain, J. M. Rehg, and E. A. Theodorou, "Aggressive driving with model predictive path integral control," in *2016 IEEE International Conference on Robotics and Automation (ICRA)*, 2016, pp. 1433–1440.
- [2] ———, "Information-theoretic model predictive control: Theory and applications to autonomous driving," *IEEE Transactions on Robotics*, vol. 34, no. 6, pp. 1603–1622, 2018.
- [3] E. Trevisan and J. Alonso-Mora, "Biased-mppi: Informing sampling-based model predictive control by fusing ancillary controllers," *IEEE Robotics and Automation Letters*, vol. 9, no. 6, pp. 5871–5878, 2024.
- [4] I. S. Mohamed, J. Xu, G. S. Sukhatme, and L. Liu, "Towards efficient mpqi trajectory generation with unscented guidance: U-mpqi control strategy," *IEEE Transactions on Robotics*, 2025.
- [5] Q. Liu and D. Wang, "Stein variational gradient descent: A general purpose bayesian inference algorithm," *Advances in neural information processing systems*, vol. 29, 2016.
- [6] A. Lambert, A. Fishman, D. Fox, B. Boots, and F. Ramos, "Stein variational model predictive control," *arXiv preprint arXiv:2011.07641*, 2020.
- [7] T. Miura, N. Akai, K. Honda, and S. Hara, "Spline-interpolated model predictive path integral control with stein variational inference for reactive navigation," in *2024 IEEE International Conference on Robotics and Automation (ICRA)*. IEEE, 2024, pp. 13 171–13 177.
- [8] K. Honda, N. Akai, K. Suzuki, M. Aoki, H. Hosogaya, H. Okuda, and T. Suzuki, "Stein variational guided model predictive path integral control: Proposal and experiments with fast maneuvering vehicles," in *2024 IEEE International Conference on Robotics and Automation (ICRA)*. IEEE, 2024, pp. 7020–7026.
- [9] K. Holkar and L. M. Waghmare, "An overview of model predictive control," *International Journal of control and automation*, vol. 3, no. 4, pp. 47–63, 2010.
- [10] M. Morari and J. H. Lee, "Model predictive control: past, present and future," *Computers & chemical engineering*, vol. 23, no. 4-5, pp. 667–682, 1999.
- [11] G. Williams, B. Goldfain, P. Drews, K. Saigol, J. M. Rehg, and E. A. Theodorou, "Robust sampling based model predictive control with sparse objective information," in *Robotics: Science and Systems*, vol. 14, 2018, p. 2018.
- [12] I. M. Balci, E. Bakolas, B. Vlahov, and E. A. Theodorou, "Constrained covariance steering based tube-mppi," in *2022 American Control Conference (ACC)*, 2022, pp. 4197–4202.
- [13] M. S. Gandhi, B. Vlahov, J. Gibson, G. Williams, and E. A. Theodorou, "Robust model predictive path integral control: Analysis and performance guarantees," *IEEE Robotics and Automation Letters*, vol. 6, no. 2, pp. 1423–1430, 2021.
- [14] Y. Qu, H. Chu, S. Gao, J. Guan, H. Yan, L. Xiao, S. E. Li, and J. Duan, "RI-driven mpqi: Accelerating online control laws calculation with offline policy," *IEEE Transactions on Intelligent Vehicles*, vol. 9, no. 2, pp. 3605–3616, 2023.
- [15] P. Wang, C. Li, C. Weaver, K. Kawamoto, M. Tomizuka, C. Tang, and W. Zhan, "Residual-mppi: Online policy customization for continuous control," *arXiv preprint arXiv:2407.00898*, 2024.
- [16] M. D. Hoffman, D. M. Blei, C. Wang, and J. Paisley, "Stochastic variational inference," *the Journal of machine Learning research*, vol. 14, no. 1, pp. 1303–1347, 2013.

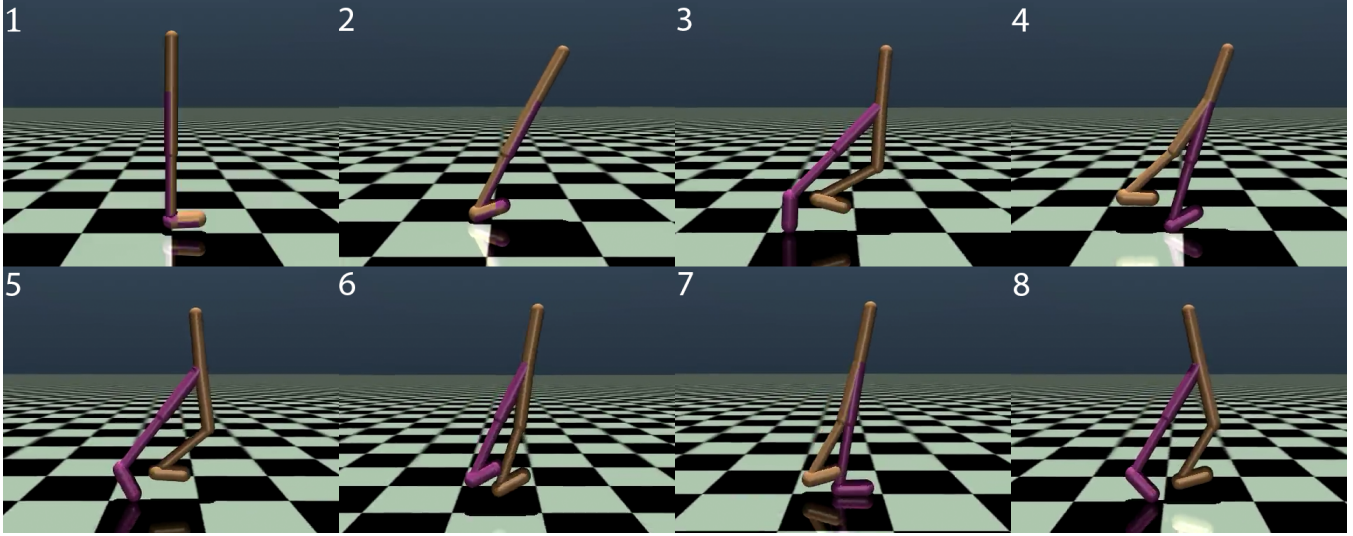


Fig. 5. Sample 2D walker gait from initial position. Events are sequenced in ascending numerical order. The reference gait encouraged a "skipping" motion which results in several instances of the walker not touching the ground plane.

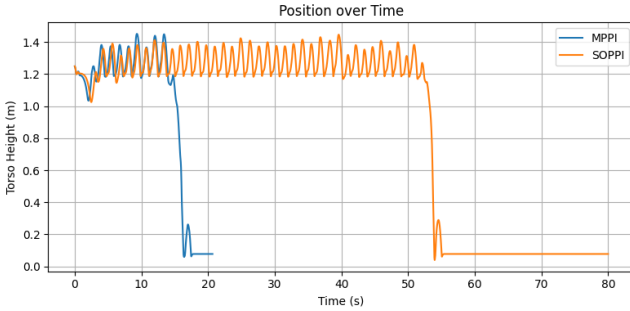


Fig. 6. SOPPI vs. MPPI on the 2D walking task - median length trial for each algorithm

- [17] Y. Aoyama, P. Lehmann, and E. A. Theodorou, "Second-order stein variational dynamic optimization," *arXiv preprint arXiv:2409.04644*, 2024.
- [18] T. Power and D. Berenson, "Constrained stein variational trajectory optimization," *IEEE Transactions on Robotics*, vol. 40, pp. 3602–3619, 2024.
- [19] J. Pavlasek, J. Mah, O. Jenkins, and F. Ramos, "Stein variational belief propagation for decentralized multi-robot control," in *Workshop on Distributed Graph Algorithms for Robotics at ICRA 2023*, 2023.
- [20] J. Pavlasek, J. J. Z. Mah, R. Xu, O. C. Jenkins, and F. Ramos, "Stein variational belief propagation for multi-robot coordination," *IEEE Robotics and Automation Letters*, vol. 9, no. 5, pp. 4194–4201, 2024.
- [21] J. Ansel, E. Yang, H. He, N. Gimelshein, A. Jain, M. Voznesensky, B. Bao, P. Bell, D. Berard, E. Burovski, G. Chauhan, A. Chourdia, W. Constable, A. Desmaison, Z. DeVito, E. Ellison, W. Feng, J. Gong, M. Gschwind, B. Hirsh, S. Huang, K. Kalambarkar, L. Kirsch, M. Lazos, M. Lezcano, Y. Liang, J. Liang, Y. Lu, C. Luk, B. Maher, Y. Pan, C. Puhrsch, M. Reso, M. Saroufim, M. Y. Siraichi, H. Suk, M. Suo, P. Tillet, E. Wang, X. Wang, W. Wen, S. Zhang, X. Zhao, K. Zhou, R. Zou, A. Mathews, G. Chanan, P. Wu, and S. Chintala, "PyTorch 2: Faster Machine Learning Through Dynamic Python Bytecode Transformation and Graph Compilation," in *29th ACM International Conference on Architectural Support for Programming Languages and Operating Systems, Volume 2 (ASPLOS '24)*. ACM, Apr. 2024. [Online]. Available: <https://docs.pytorch.org/assets/pytorch2-2.pdf>
- [22] E. Todorov, T. Erez, and Y. Tassa, "Mujoco: A physics engine for

- model-based control," in *2012 IEEE/RSJ International Conference on Intelligent Robots and Systems*. IEEE, 2012, pp. 5026–5033.
- [23] M. Towers, A. Kwiatkowski, J. Terry, J. U. Balis, G. De Cola, T. Deleu, M. Goulão, A. Kallinteris, M. Krimmel, A. KG, et al., "Gymnasium: A standard interface for reinforcement learning environments," *arXiv preprint arXiv:2407.17032*, 2024.
- [24] R. Newbury, J. Collins, K. He, J. Pan, I. Posner, D. Howard, and A. Cosgun, "A review of differentiable simulators," *IEEE Access*, 2024.
- [25] C. D. Freeman, E. Frey, A. Raichuk, S. Girgin, I. Mordatch, and O. Bachem, "Brax - a differentiable physics engine for large scale rigid body simulation," 2021. [Online]. Available: <http://github.com/google/brax>
- [26] M. Macklin, "Warp: A high-performance python framework for gpu simulation and graphics," <https://github.com/nvidia/warp>, March 2022, nVIDIA GPU Technology Conference (GTC).
- [27] R. Mukhopadhyay, R. Chaki, A. Sutradhar, and P. Chattopadhyay, "Model learning for robotic manipulators using recurrent neural networks," in *TENCON 2019-2019 IEEE Region 10 Conference (TENCON)*. IEEE, 2019, pp. 2251–2256.
- [28] R. V. Florian, "Correct equations for the dynamics of the cart-pole system," *Center for Cognitive and Neural Studies (Coneural), Romania*, vol. 63, 2007.
- [29] M. AOKI, "Python simple mppi," 2025. [Online]. Available: https://github.com/MizuhoAOKI/python_simple_mppi
- [30] D. Berenson, M. Van der Merwe, and Z. Huang. [Online]. Available: <https://berenson.robtics.umich.edu/courses/winter2025robotlearning/index.html>
- [31] J. Alvarez-Padilla, J. Z. Zhang, S. Kwok, J. M. Dolan, and Z. Manchester, "Real-time whole-body control of legged robots with model-predictive path integral control," in *2025 IEEE International Conference on Robotics and Automation (ICRA)*. IEEE, 2025, pp. 14 721–14 727.
- [32] J. Schulman, F. Wolski, P. Dhariwal, A. Radford, and O. Klimov, "Proximal policy optimization algorithms," *CoRR*, vol. abs/1707.06347, 2017. [Online]. Available: <http://arxiv.org/abs/1707.06347>
- [33] A. Raffin, A. Hill, A. Gleave, A. Kanervisto, M. Ernestus, and N. Dormann, "Stable-baselines3: Reliable reinforcement learning implementations," *Journal of Machine Learning Research*, vol. 22, no. 268, pp. 1–8, 2021. [Online]. Available: <http://jmlr.org/papers/v22/20-1364.html>